

FEMTOSECOND X-RAYS FROM 90° THOMSON SCATTERING*

W. Leemans, R. Schoenlein, A. Chin, E. Glover, R. Govil, P. Volfbeyn, S. Chattopadhyay, K.- J. Kim, and C. V. Shank, Lawrence Berkeley Laboratory, Berkeley, CA 94720 USA

We report on progress on the femtosecond X-ray pulse generation experiment. The experiment involves a relativistic electron beam (50 MeV) with an rms bunch length of 10 ps containing 1 - 2 nC of charge, and a ultrashort pulse (50 - 200 fs), high power (< 4 TW) $0.8 \mu\text{m}$ laser beam from a Ti:Al₂O₃ laser system. Both beams are focused down to about a $50 \mu\text{m}$ waist size and intersect at 90°. The laser field acts as an electromagnetic undulator for the relativistic electron beam generating radiation upshifted by $2\gamma^2$ and a pulse length given by the transit time of the laser beam across the electron beam. For a 50 MeV electron beam we expect 10^5 photons at 0.4 \AA (25% bandwidth) in a cone angle of 6 - 10 mrad in about a 200 fs pulse.

I. INTRODUCTION

Scattering of femtosecond laser pulses off a low energy relativistic electron beam at 90° offers the possibility to generate ultrashort X-ray pulses. Experiments are under way in the Beam Test Facility of the Center for Beam Physics at LBL to demonstrate the generation, detection and practical utility of such pulses. The laser field acts as an electromagnetic undulator generating up-shifted radiation and, in this geometry, the x-ray pulse length is determined by the overlapped interaction length in time of the laser beam and the electron beam [1].

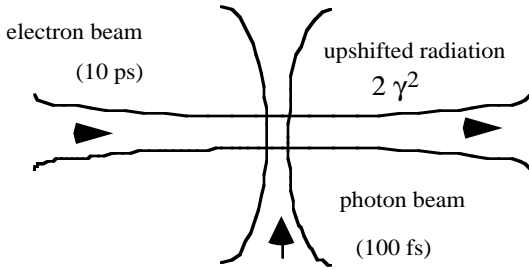


Figure 1: A generic lay-out of the 90° x-ray generation experiment. The laser beam is upshifted by $2\gamma^2$ and propagates in the direction of the electron beam.

We have previously reported on the design of this experiment which involves a relativistic electron beam and a high intensity short pulse laser [2]. The generic set-up is shown in Fig. 1. We next describe the details of the linac, laser system and experimental set-up, followed by up-to-date results of the experiment.

II. EXPERIMENT DESCRIPTION

* Supported by the Director, Office of Energy Research, Office of High Energy and Nuclear Physics, High Energy Physics Division, of the U. S. Department of Energy under Contract No. DE-AC03-76SF00098.

A. Electron Transport Line and Laser Beam Parameters

The experiment is conducted at the Beam Test Facility (BTF) which has been constructed by the Center for Beam Physics and is operated by the Center in support of its experimental R&D program. The BTF houses an electron beam transport line which transports the 50 MeV electron beam from the Advanced Light Source (ALS) into a dedicated experimental cave, and a terawatt laser system [3]. The measured electron beam parameters are given in Table 1.

Maximum Energy	50 MeV
Charge	1-2 nC/bunch
Bunch Length (σ_z)	10-15 ps
Emittance rms (unnorm)	0.35 mm-mrad
bunches/macropulse @ 125 MHz	1 - 10 (max 100)
Macropulse rep. rate	1 - 10 Hz

Table 1: Electron beam parameters

The transport line is equipped with two integrating current transformers for charge transport efficiency measurements, high bandwidth beam position monitors, fluorescent screens for transverse beam analysis and an optical transition radiation (OTR) diagnostic system [4]. The OTR system allows single bunch measurement of beam emittance, energy, and bunch length.

The main laser system parameters have been measured and are listed in Table 2.

Wavelength	$0.8 \mu\text{m}$
Energy/pulse	125 mJ
Pulse length	50 - 200 fs
Repetition rate	10 Hz
Timing jitter with respect to e-beam	2 ps

Table 2: Ti:Al₂O₃ laser system parameters.

The passively Kerr lens modelocked Ti:Al₂O₃ laser oscillator operates at 125 MHz (4th subharmonic of the ALS 500 MHz linac masterclock frequency). After stretching the oscillator pulses by a factor 10^4 , a single pulse is selected and amplified through an 8-pass pre-amplifier and a 4 pass main amplifier. The pulse is compressed in a vacuum compressor to a nominal pulse width of 100 fs (FWHM) containing an energy of about 100 mJ. The beam is propagated into the BTF cave and focused with a spherical mirror.

B. X-ray source parameters

Theoretical properties of the X-ray source have been previously described [1, 2]. The frequency of the upshifted

radiation can easily be calculated from energy and momentum conservation:

$$\omega_r \cong \frac{2\gamma^2\omega_0}{1+K^2/2+\gamma^2\theta^2} \quad (1)$$

where the Compton shift has been neglected. Here γ is the Lorentz factor, K the wiggler strength, θ the angle of observation and ω_0 the incident laser frequency. The wiggler strength is given by

$$K = \frac{25.6}{c[\text{cm/s}]} \sqrt{I[\text{W/cm}^2]\lambda[\mu\text{m}]} \quad (2)$$

where I is the incident laser intensity and λ the laser wavelength. From Eqn. (2) it is clear that wavelength tuning can be achieved by reducing the laser spot size at the interaction point to obtain wiggler strengths on the order of 1. Since the x-ray yield depends linearly on the laser energy no photon flux reduction is expected. In addition, harmonic generation is expected to become important at such large wiggler strengths [5].

For our experimental parameters, the x-ray pulse width, bandwidth and total flux are calculated from the expressions given by Kim et al. [1] and are listed in Table 3.

Wavelength (Å)	0.4
Pulse length (fs)	200
# photons (25 % bandwidth)	1×10^5
Full angle cone (mrad)	6
Bandwidth (%)	25

Table 3: x-ray source parameters.

The main contributions to the bandwidth are from the finite electron beam emittance and limited number of wiggler periods seen by the electrons. The finite emittance effect causes a washing out of the typical angularly correlated wavelength distribution for a single radiating electron. Neglecting the finite wiggler period effect, the actual source bandwidth is obtained by taking the convolution of the single electron radiation pattern with a Gaussian distribution for the angles that the electrons make with respect to the laser beam. For a beam emittance of 0.35 mm-mrad and a spot size of 50 μm , the electron beam divergence is 6 mrad which leads to an intrinsic bandwidth on the order of 20 - 25 %.

III. EXPERIMENTAL RESULTS

We next describe in detail the main milestones that have been passed on the way towards generating femtosecond x-ray pulses.

A. Electron Beam Focused to less than 100 μm .

The electron beam has been focused down to a spot size less than 100 μm using a telescope consisting of two quadrupole triplets. The large bore (6") of the final magnet allows for small f-number focusing and reduces Bremsstrahlung production by beam halo scraping against the beam pipe. The electron beam profile at the interaction point

has been measured using OTR and is shown in Fig. 2. The pointing stability was found to be better than 50 μm .

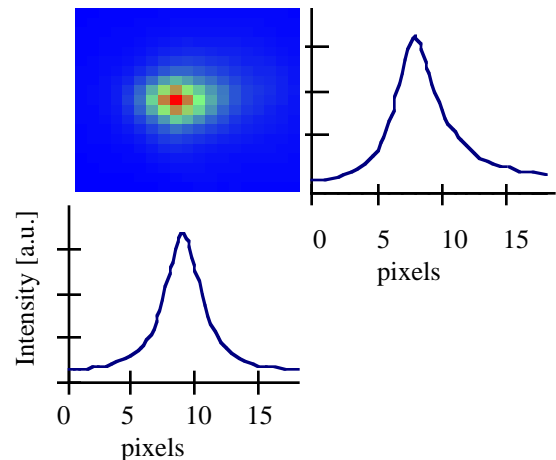


Figure 2: OTR image of the electron beam spot inside the X-ray interaction chamber with vertical (right) and horizontal (bottom) line-out. The actual spot size is probably less than the measured spot size $\sigma_x = 115$ as the present optical lens system is resolution limited to about 100 μm .

B. Electron and Laser Beam Synchronized

To ensure proper synchronization between the laser and the electron beam, a feedback system has been implemented to continually adjust the laser oscillator cavity frequency. The laser oscillator operates at 125 MHz (1/4 of the 500 MHz linac frequency). A 500 MHz signal synchronous with the laser oscillator is extracted from a photodiode signal using a 500 MHz bandpass filter. An error signal, which drives a piezo-controlled mirror mount, is then obtained by mixing this 500 MHz signal with the 500 MHz linac reference signal.

Using a streak camera with picosecond time resolution we have verified that locking of the laser oscillator to the electron beam was achieved with timing jitter performance of about 2 ps (Fig. 3).

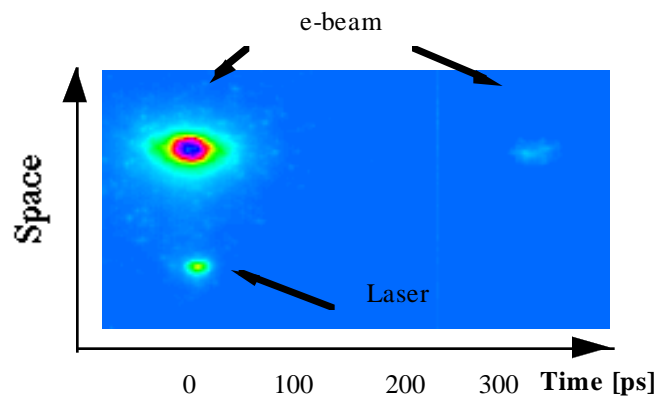


Figure 3: Time resolved streak camera image showing OTR radiation from the electron beam (main bunch and trailing bunch separated by 333 ps) and laser beam fiducial.

Optical transition radiation from the electron beam and laser oscillator pulses were simultaneously imaged onto the slit of the streak camera. A histogram of 50 consecutive shots is shown in Fig. 4.

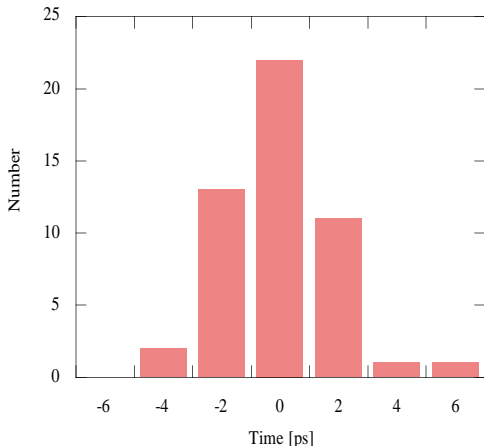


Figure 4: Histogram of separation in time between electron beam and laser beam as measured from streak camera images such as the one shown in Fig. 3.

An on-line timing signature of the electron beam and of the laser beam is obtained from a high bandwidth beam position monitor and an ultra-high speed photo-diode respectively. The 6 ps rise time diode detects laser light leaking through the final focusing mirror. Both those signals are then combined and monitored on a Tektronix SCD 5000 oscilloscope.

C. X-ray Measurements

A variety of x-ray diagnostics are being implemented and developed to measure wavelength, beam size and divergence, pulse length and polarization of the produced x-ray beam.

A 60° H-magnet separates the particle and photon beams after the interaction point. A 75 μm Be-foil isolates the beam line (high vacuum) from the x-ray diagnostic systems.

Spatial properties of the X-ray beam (spot size and divergence) are being measured using a slow scan CCD camera looking at a phosphor screen. Preliminary results using this phosphor indicate that the total x-ray background contribution (mainly due to Bremsstrahlung) is about two orders of magnitude below the expected signal level..

To determine the angular wavelength distribution of the x-ray photon beam we are using a 1 cm thick, 3 cm diameter cooled Ge-detector. The detector has been calibrated using the 26 keV and 60 keV emission lines from an Am²⁴¹ source and has about a 2.5 % energy resolution at 30 keV. Since this detector is capable of detecting single photons, background levels need to be kept below a single photon per pulse for operating this detector. A 1 mm diameter, 2 cm long lead

pinhole is used to spatially filter the background x-ray radiation incident on the detector and to reduce the signal level to a single x-ray photon per shot to avoid pile-up.

For initial pulse length measurements the transit time will be lengthened by changing the horizontal focusing strength of the quadrupoles, allowing the use of a diamond photodiode as well as an X-ray streak camera. A coincidence technique between the X-ray pulse and an optical pulse in a gas jet is being developed to measure shorter pulse durations [6]. In the absence of the laser, photo electrons will be produced in a Kr gas jet by tuning the source to produce 14.8 keV x-rays, about 500 eV higher than the K-shell energy of Kr-gas (14.3 keV). If the laser pulse arrives simultaneously with the x-ray pulse, the x-ray photo electrons will acquire an additional drift velocity component whose magnitude and direction depends on the phase and amplitude of the laser field at which the photo electron is born and the relative polarization of the laser with respect to the x-rays. The temporal overlap between the two pulses will therefore determine the emitted x-ray photo electron spectrum.

IV. SUMMARY

A status report has been given of the orthogonal Thomson scattering experiment at the BTF. Based on simple scaling laws we expect that about 10⁵ x-ray photons with an energy of 30 keV will be produced for our current experimental parameters. Both the electron beam line and the laser system have been completed. The electron beam has been focused to a spot size less than 100 μm. The 25 ps (FWHM) electron and 100 fs (FWHM) laser pulses have been synchronized to a jitter level of about 2 ps. We have started looking at x-ray generation using a phosphor screen imaged onto a slow scan CCD camera as well as a Ge-detector and are poised to start intense x-ray measurements in the coming months.

V. ACKNOWLEDGMENTS

The authors wish to thank the ALS personnel for their help in the construction and operation of the Beam Test Facility, in particular Dennis Calais and Terry Byrne. We would also like to thank Leon Archambault for his engineering and technical support and Harvey Gould, Ali Belkacem and Norm Madden for their help with the Ge-detector.

VI. REFERENCES

- [1] K.- J. Kim et al., NIMA 341, 351 (1994).
- [2] W. Leemans et al., AIP Proc. 1994 Workshop on Advanced Accelerator Concepts, Lake Geneva, LBL-36369.
- [3] W. Leemans et al., IEEE Proc. 1993 Part. Accel Conf, 83 (1993) and Proc. 1994 European Part. Accel. Conf.
- [4] M. de Loos et al., Proc. 1994 European Part. Accel. Conf.
- [5] E. Esarey et al., Phys. Rev E **48**, 3003 (1993).
- [6] J.M. Schins et al., Phys. Rev. Lett 73, 2180 (1993).